1226–1239 *Nucleic Acids Research, 2012, Vol. 40, No. 3* *Published online 12 October 2011*
doi:10.1093/nar/gkr800

An essential role for Clp1 in assembly of polyadenylation complex CF IA and Pol II transcription termination

Raphaël Haddad[1,2], Frédérique Maurice[1,3], Nicolas Viphakone[1,2], Florence Voisinet-Hakil[1,2], Sébastien Fribourg[1,3] and Lionel Minvielle-Sébastia[1,2,3,*]

[1]Université Bordeaux Segalen, [2]CNRS, UMR5095, IBGC, Bordeaux, F-33000 and [3]INSERM, U869, Laboratoire ARNA, Pessac, F-33600, France

Received April 25, 2011; Revised and Accepted September 12, 2011

ABSTRACT

Polyadenylation is a co-transcriptional process that modifies mRNA 3′-ends in eukaryotes. In yeast, CF IA and CPF constitute the core 3′-end maturation complex. CF IA comprises Rna14p, Rna15p, Pcf11p and Clp1p. CF IA interacts with the C-terminal domain of RNA Pol II largest subunit via Pcf11p which links pre-mRNA 3′-end processing to transcription termination. Here, we analysed the role of Clp1p in 3′ processing. Clp1p binds ATP and interacts in CF IA with Pcf11p only. Depletion of Clp1p abolishes transcription termination. Moreover, we found that association of mutations in the ATP-binding domain and in the distant Pcf11p-binding region impair 3′-end processing. Strikingly, these mutations prevent not only Clp1p-Pcf11p interaction but also association of Pcf11p with Rna14p-Rna15p. ChIP experiments showed that Rna15p cross-linking to the 3′-end of a protein-coding gene is perturbed by these mutations whereas Pcf11p is only partially affected. Our study reveals an essential role of Clp1p in CF IA organization. We postulate that Clp1p transmits conformational changes to RNA Pol II through Pcf11p to couple transcription termination and 3′-end processing. These rearrangements likely rely on the correct orientation of ATP within Clp1p.

INTRODUCTION

Polyadenylation is a co-transcriptional event that occurs at the 3′-end of nearly all eukaryotic mRNA precursors (1,2). This essential maturation process starts with cleavage of the elongating pre-mRNA in the 3′-untranslated region (3′-UTR) followed by the addition of a poly(A) tract at the 3′-hydroxyl end of the upstream cleavage product. The endonucleolytic cleavage also generates a 5′-phosphorylated RNA downstream of the poly(A) site that provides an entry site for the exonuclease Rat1 (in yeast)/Xrn2(in human) which subsequently degrades this RNA. This exonucleolytic degradation is part of a complex mechanism that triggers termination of transcription in eukaryotes (3–5). Pre-mRNA processing and subsequent termination of transcription rely on the recognition of polyadenylation-specific sequences on the primary transcript by the polyadenylation machinery. The 3′-end processing complex is now well described in both yeast and mammals (6–8). In *Saccharomyces cerevisiae*, the first factor that was identified at the level of its subunit composition was the cleavage/polyadenylation factor IA (CF IA), involved in both the cleavage and polyadenylation steps (9,10). The polyadenylation complex also comprises the large cleavage and polyadenylation factor [CPF, with up to 15 different subunits identified; (11–13)], the RNA-binding protein Hrp1p/Nab4p (14,15) and the poly(A)-binding proteins Pab1p and Nab2p, involved in the control of poly(A) tail synthesis and subsequent export of the mature mRNA (10,16–18). Multiple protein–protein interactions have been identified between subunits of the factors (6,7).

CF IA consists of Rna14p, Rna15p, Pcf11p and Clp1p. Rna14p and Rna15p interact tightly with each other (19) and with Pcf11p (20,21). Rna15p is an RNA-binding protein that cooperates with Hrp1p/Nab4p to specifically bind the positioning and efficiency elements located upstream of the cleavage site (22). Pcf11p is required for both

*To whom correspondence should be addressed. Tel/Fax: +33 5 4000 2213; Email: lionel.minvielle@inserm.fr
Present addresses:
Raphaël Haddad, ExonHit Therapeutics SA, F-75013, Paris.
Nicolas Viphakone, Department of Molecular Biology and Biotechnology, University of Sheffield, Sheffield, UK.
Florence Voisinet-Hakil, CNRS, IPREM, UMR 5254, Pau, F-64013, France.

pre-mRNA 3′-end processing and transcription termination. Its N-terminus interacts specifically with the carboxyl-terminal domain (CTD) of the largest subunit of RNA polymerase II (Pol II), while the central and C-terminal regions of Pcf11p contact Rna14p/Rna15p and Clp1p, respectively (23). The CTD-interacting domain (CID) of Pcf11p is dispensable for 3′-end processing *in vitro* but is essential to avoid transcriptional readthrough *in vivo* (23,24).

It has been reported that Clp1p, upon *in vitro* reconstitution of the factor with recombinant proteins, associates with CF IA via Pcf11p, making no contacts with either Rna14p or Rna15p (21). Although all four subunits appeared to be required as a complex to fulfil CF IA essential function in 3′ processing (21), no precise role has been attributed to Clp1p in this maturation process. First identified in yeast as the fourth subunit of CF IA (10), Clp1 orthologue was subsequently found associated with hPcf11 in a mammalian factor called Cleavage Factor II (CF II_m) (25). Interestingly, yeast CF IA is required for both cleavage and polyadenylation whereas CF II_m acts in cleavage only. Consistent with the presence of a conserved P-loop/Walker A motif in its sequence, Clp1p binds ATP (26). Recently, human Clp1 (hClp1) has been shown to work in the yeast-like pathway of tRNA splicing and activate synthetic siRNAs *in vitro* (27,28). In addition, expression of hClp1 or its archeal orthologue *Pho*Clp1 (from *Pyrococcus horikoshii*) can complement a kinase-defective mutant of the essential yeast tRNA ligase *TRL1* (27–29). However, hClp1 cannot compensate for the loss of yeast *CLP1* expression (27,28). Despite its structural similarity with hClp1 (26), yeast Clp1p has no detectable ATPase activity (26–28). Since the kinase activity for RNA healing in tRNA splicing is carried out by the multifunctional Trl1 protein (30) and given that no siRNA pathway exists in budding yeast, it is unlikely that hClp1 and yeast Clp1p are functional homologues. Therefore, we anticipate that Clp1p may exert its essential function in pre-mRNA 3′-end processing only.

In this study, we investigated the role of Clp1p in mRNA 3′-end formation. Taking advantage of the yeast system, we looked for conditional lethal mutants that exhibit temperature-sensitive (Ts) phenotypes at 37°C. We found that these mutations affect cleavage and polyadenylation *in vitro*. Depletion of Clp1p and Pcf11p *in vivo* resulted in transcription termination defects at snoRNA transcription units. Importantly, the association of Rna14p/Rna15p to Pcf11p is altered in *clp1* Ts mutants. We propose that the essential function of Clp1p in yeast is to maintain CF IA organization in order to allow the coupling of 3′-end processing and transcription termination.

MATERIALS AND METHODS

Wild-type *CLP1* plasmid constructs

The open reading frame (ORF) of the *CLP1* gene was amplified by PCR from BMA64 strain genomic DNA (Supplementary Table S1; 31) with gene-specific primers designed to introduce NotI sites upstream and downstream of the start and stop codons. The fragment was cloned into the NotI site of the yeast shuttle vectors pHH2 (*ARS-CEN, URA3*) and pAHH2 (*ARS-CEN, ADE2*), allowing the expression of a fusion Clp1 protein tagged at its N-terminus with the HA epitope-6xHistidine tag, under the control of the constitutive *CYC1* promoter and *PGK1* terminator. A longer fragment around *CLP1* ORF was amplified by PCR from wild-type genomic DNA starting from position −250 (the A of the start codon being +1) and ending at position +1650 (312 nt after the stop codon). This fragment was cloned into plasmid pFL38 [*ARS-CEN, URA3*; (32)] and pASZ11 [*ARS-CEN, ADE2*; (33)]. The constructs (pHH2-*CLP1,* pAHH2-*CLP1*, pFL38-*CLP1* and pASZ11-*CLP1*) were sequenced to control that no undesired mutation were introduced by PCR.

Construction of *CLP1*-deleted strains

Deletion of the entire ORF of the *CLP1* gene was done in the diploid BMA64(2n) strain using a technique already described (34) with either *TRP1* or *LEU2* genes as selectable markers. Correct integration was checked by PCR. Tetrad analysis after meiosis showed a segregation of 2 Trp^- (or Leu^-) viable spores and two lethal spores, the latter corresponding to *clp1::TRP1* (or *clp1::LEU2*) gene deletion, demonstrating that *CLP1* is essential for viability. The diploid strains heterozygous for the deletions were transformed with pHH2-*CLP1* or pFL38-*CLP1* and sporulated to yield haploid strains YLM127 and YLM172 (Supplementary Table S1). Most of the strains used in this study were derived from YLM127 and YLM172 by plasmid shuffling.

Construction of mutant *clp1* and *pcf11* alleles

Error-prone PCR mutagenesis was performed with plasmid pAHH2-*CLP1* as template. The PCR reaction was carried out in the presence of the specific primers used to amplify and clone *CLP1* ORF in pAHH2-*CLP1*, and 40 μM of dATP, 200 μM of each dCTP, dGTP and dTTP and *Taq* DNA polymerase. Amplified fragments were recloned into pAHH2 empty vector and used to transform YLM127 strain. Hydroxylamine mutagenesis was performed on pASZ11-*CLP1* according to Sikorski and Boeke (35). Mutagenized plasmids were used to transform YLM172. All transformants of YLM127 and YLM172 were spread 5-FOA plates to select against the *URA3 CLP1*-containing plasmids. Viable colonies were tested then for temperature-sensitivity at 37°C. The original strains YLM130 (*clp1-12* allele) and YLM179 (*clp1-5* allele) were obtained through these screens. The other *clp1* alleles used in this study (Figure 1; Supplementary Table S1) were derived from *clp1-12* and *clp1-5* by sub-cloning or site-directed mutagenesis of plasmids, transformed into YLM172 and plated on 5-FOA medium to chase the plasmid-borne wild-type allele. Serial dilutions of the resulting transformants were tested on rich medium for temperature-sensitivity at 37°C. To generate the R-Clp1p and R-Pcf11p expressing strain (YRH78 and YRH79, respectively), the GAL promoter and the ubiquitin–arginine coding sequence were fused to their ORFs on the chromosome as described (36).

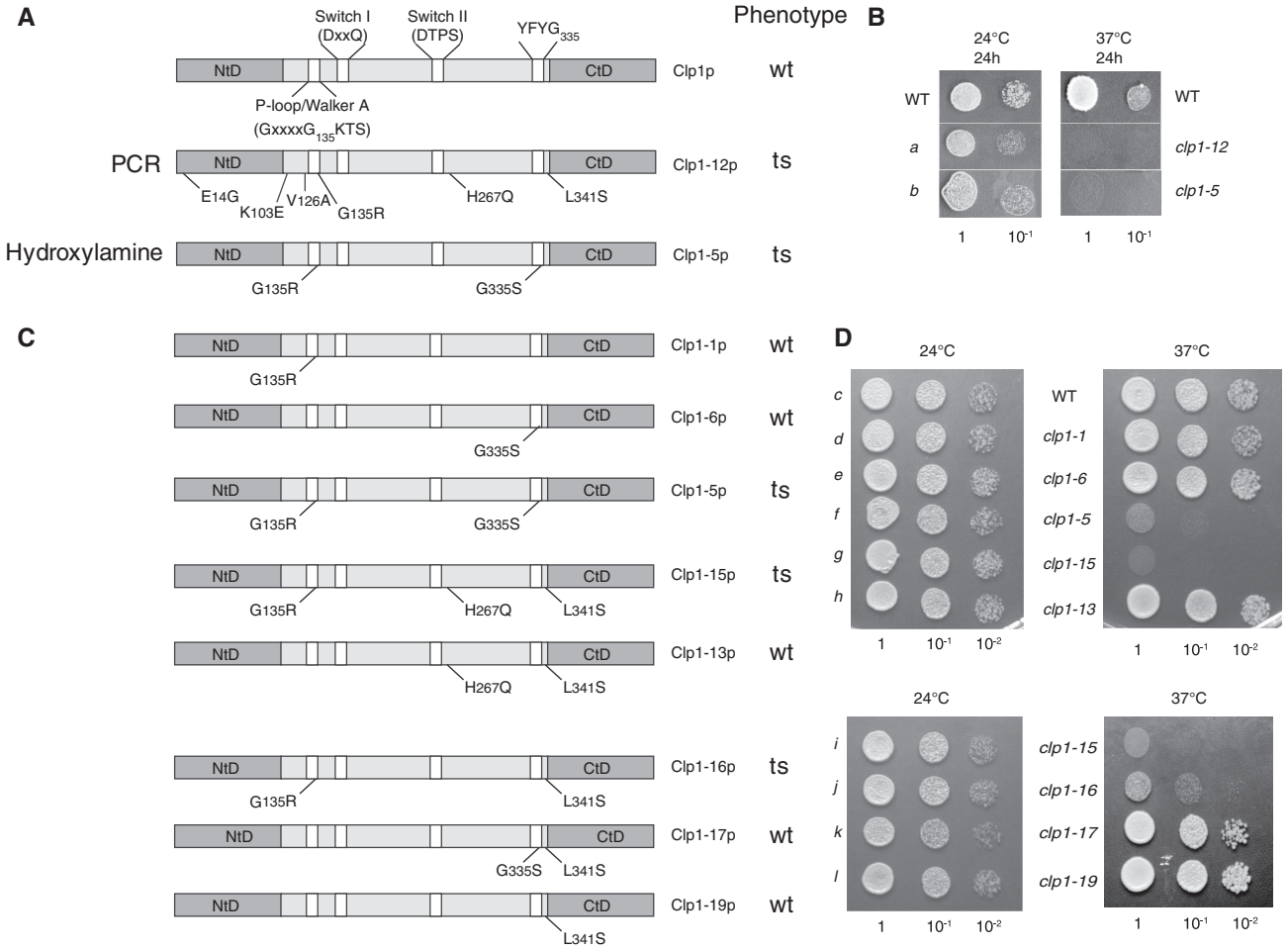

Figure 1. Phenotypic analysis of the different *clp1* alleles used in this study. (**A**) Schematic representation of the Ts alleles of the *CLP1* gene isolated after random PCR mutagenesis (*clp1-12*) or hydroxylamine mutagenesis (*clp1-12*). The conserved residues constituting the canonical P-loop/Walker A domain and the Switch loops of Clp1p are depicted on the wild-type protein, between the N-terminal (NtD) and C-terminal (CtD) domains (see also Supplementary Figure S1). Location of amino acid changes within the Ts alleles are indicated. (**B**) Ten-fold dilution of the wild-type and original *clp1-12* and *clp1-5* mutant strains were spotted on rich medium and incubated for 1 day at 24°C and 37°C. (**C**) Diagrammatic drawing of the different alleles derived from the original *clp1-5* and *clp1-12* mutants. (**D**) Ten-fold serial dilutions of the wild-type and mutant strains spotted as in (**B**) but incubated for 3 days at the indicated temperatures.

Pre-mRNA 3′-end processing assays and transcription run-on analysis

Cleavage and polyadenylation assays were done as previously described with either extracts or purified factors prepared from wild-type and mutant stains with the *CYC1* and *CYC1* pre-cleaved RNAs. Hrp1p/Nab4p and Nab2p were recombinant proteins expressed in *Escherichia coli* (17,37) Transcription run-on analysis were as described in Dheur *et al*. (36). Reverse transcription was performed on 10 µg of total RNA extracted from (i) R-Clp1p and R-Pcf11p-expressing strains 4 h after cells were shifted from galactose to glucose medium, or (ii) after a 2-h shift to 37°C for *rna15-1* and *pti1-2* mutants strains. Products were analysed on 6% polyacrylamide−8.3% urea gels.

Purification of 3′-end processing factors and recombinant proteins

Yeast factors were purified from the TAP-tagged yeast strains (Supplementary Table S1) as published (38). Purified factors were used for 3′ processing assays *in vitro* or run on 10% polyacrylamide-SDS gels, stained with silver or immunoblotted. Recombinant proteins were produced in *E. coli* BL21(DE3) cells. PCR products of the different *clp1* alleles were cloned into a pET28-derived vector and into a modified pET-15b plasmid, introducing a His_6-tag at the N-terminus of the $Pcf11^{(454–563)}$ protein. Bacterial cells were co-transformed with $Pcf11p^{(454-563)}$- and Clp1p-expressing plasmids, grown at 37°C and further induced overnight with 1 mM IPTG at 15°C. Co-precipitations were performed as described (39).

Chromatin immunoprecipitation

Chromatin immunoprecipitations (ChIPs) were done with TAP-tagged proteins and quantitative PCR amplification of the immunoprecipitated (IP) fragments were performed with primers corresponding to the *ADH1* gene as described (40–42). PCR reactions were run on native 8%-polyacrylamide gels. The gels were fixed, dried,

exposed to phosphorimaging screens before scanning with a Biorad Pharos machine for quantitative measurements of the IP material. Occupancies at each position were calculated by dividing the ratio of the IP over the corresponding Input DNA at each location of the *ADH1* gene, by the ratio of IP over Input of a non-transcribed region of chromosome V, as explained in (40). For easier comparisons, the value obtained with fragment number 3 for each immunoprecipitation at 24°C was set up to 100 and the other values were expressed proportionally.

RESULTS

clp1 conditional mutants define two important regions in the Clp1 protein

Although Clp1p is an essential subunit of the yeast pre-mRNA 3′-end processing machinery (10,21), its role remains unknown. In order to gain further insight into its function, we employed error-prone PCR and chemical mutagenesis to generate random mutations in the *CLP1* gene. The plasmid-borne mutant alleles were introduced by plasmid-shuffling into a strain carrying the *clp1Δ* null allele. The resulting mutant strains were tested for temperature-sensitivity and two independent mutants were identified that were unable to grow at 37°C. The *clp1-12* resulted from random PCR mutagenesis, and the *clp1-5* allele was obtained by hydroxylamine mutagenesis (Figure 1A and B). Mapping the mutations within the *clp1* mutant ORFs revealed six and two point mutations within the *clp1-12* and *clp1-5* alleles, respectively (Figure 1A). To seek out the simplest modifications that were responsible for the Ts phenotype, we separated the mutations in the two alleles. Interestingly, the combination of both mutations (G135R, G335S) was required for the Ts phenotype of the *clp1-5* mutant, as each mutation independently conferred a temperature-resistant phenotype [Figure 1C, *clp1-1* (G135R) and *clp1-6* (G335S); Figure 1D, rows *d* and *e*]. Likewise, simplification of the Ts mutant allele *clp1-12* (6 mutations) gave rise to both the Ts *clp1-15* mutant (G135R, H267Q, L341S) and the temperature-resistant *clp1-13* allele (H267Q, L341S), (Figure 1C and D, see rows *g* and *h*, respectively). Sequence inspection of Clp1 orthologues showed that G135 lies within highly conserved residues constituting the P-loop/Walker A motif. This motif is found in most ATP-/GTP-binding proteins and forms the nucleotide binding site within the central domain [Figure 1A and Supplementary Figure S1; (43)]. Specifically, the backbone amide of G135 makes direct contact with the β-phosphate group of the bound ATP (26). Given that eight additional residues are in the vicinity of the nucleotide [6 in the central domain and 2 in the N-terminal domain; (26)], it is not surprising that the G135R mutation alone did not abolish Clp1p function that may be linked to ATP binding. The second-site mutation in *clp1-5*, G335S, belongs to a perfectly conserved sequence region (YFYG) found at the interface with another CF IA essential subunit, Pcf11p [Supplementary Figure S1; (26)]. Similar to G135R, this mutation does not independently result in a Ts phenotype (in the *clp1-6* mutant). The L341S mutation, found in the *clp1-15* Ts mutant allele, also lies close to the Pcf11p interaction surface and is not capable of eliciting a Ts phenotype on its own (Figure 1C, mutant *clp1-19*, and Figure 1D, row *l*). Interestingly, combination of both G335S and L341S within the same allele (called *clp1-17*; Figure 1C) is still unable to cause a growth defect (Figure 1D, row *k*). We observed that a third mutation, H267Q, in the *clp1-15* compared to *clp1-16*, is able to intensify the Ts phenotype (Figure 1C and D, row *j*). This additional mutation very likely contributes to lowering the overall mutant protein stability which results in a more drastic temperature-sensitivity.

The genetic enhancement observed when mutations in the ATP-binding site and the Clp1p/Pcf11p-interaction region of the Clp1 protein are combined revealed that these conserved regions of the central domain of the protein are essential for Clp1p function.

mRNA 3′-end formation is impaired in *clp1* Ts mutant extracts

To explore the specific function of Clp1p in pre-mRNA 3′-end processing, we prepared whole cell extracts from a wild-type strain and from the most severely affected *clp1* mutants. We then performed standard *in vitro* pre-mRNA cleavage and polyadenylation assays on the synthetic *CYC1* pre-mRNA as described (37). Extracts made from the mutant strains showed a dramatic reduction of cleavage (Figure 2A, compare lanes 5, 8 and 10 to lanes 2, 3, 4, 6, and 9). Cleavage could be effectively restored when purified wild-type CF IA was added to the deficient extracts (Figure 2A, lane 12, 13, 14 and 18). However, complementaton with recombinant Clp1p alone is inefficient to restore productive cleavage of the precursor (Figure 2A, lanes 15–17). We next performed polyadenylation assays with the pre-cleaved *CYC1* precursor terminating at the natural poly(A) site (37). Both *clp1-5* and *clp1-12* mutant extracts were unable to polyadenylate pre-cleaved *CYC1* pre-mRNA (Figure 2B, compare lanes 3 and 6 to lanes 2). As observed for cleavage, addition of CF IA efficiently restored polyadenylation (Figure 2B, lane 5 and 8) in contrast to the poor improvement observed when recombinant Clp1p was added (Figure 2B, lane 4 and 7). These results confirm that Clp1p, only as part of CF IA, is directly involved in both steps of mRNA 3′-end formation.

In vivo depletion of Clp1p and Pcf11p affects transcription termination at *snoRNA* genes

It has been shown previously that the three components of CF IA, Rna14p, Rna15p and Pcf11p, are required for 3′-end formation of snoRNAs (42,44,45). To investigate the importance of the last CF IA subunit in this maturation process, we depleted Clp1p from cells using strains bearing the conditional allele *GAL::(Arg)-CLP1*, and used *GAL::(Arg)-PCF11* as control (Figure 3A). In such strains, the expression of Clp1p or Pcf11p can be repressed via the strong conditional *GAL10* promoter. In addition, Clp1p and Pcf11p remaining after the switch to glucose are efficiently degraded due to the presence of a

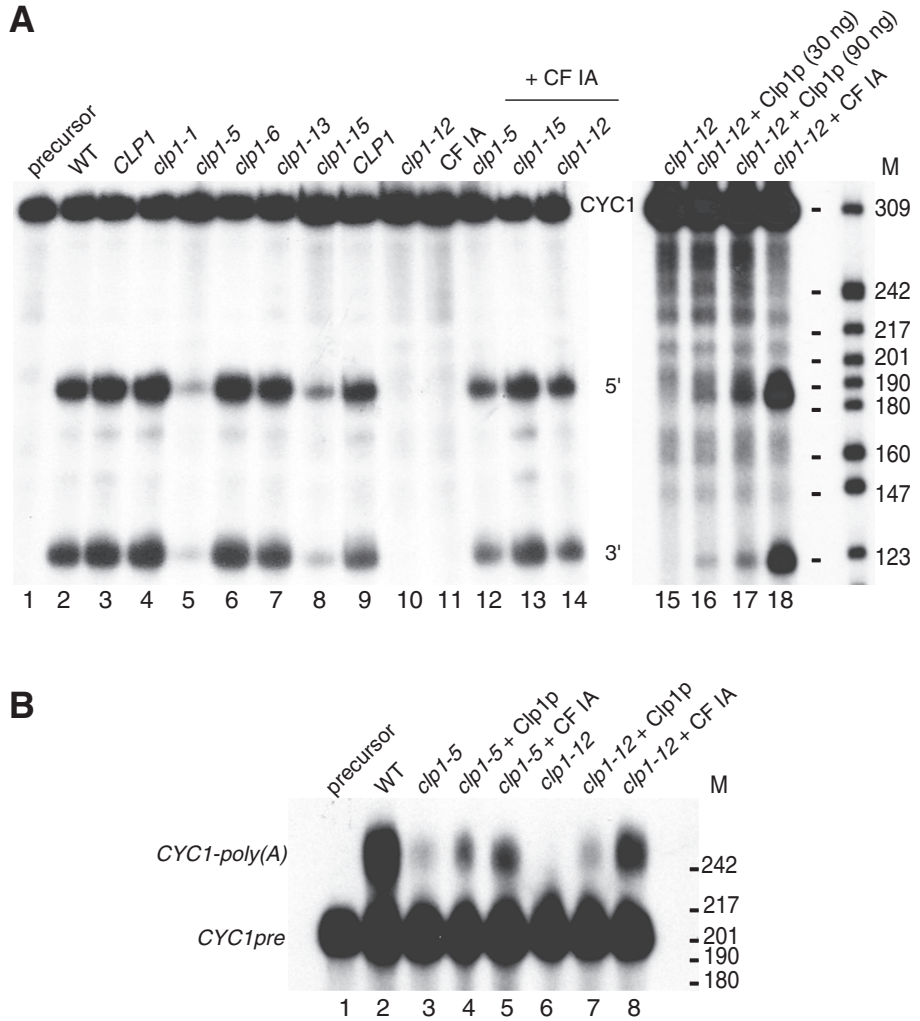

Figure 2. Clp1p is required for pre-mRNA 3′-end cleavage and polyadenylation *in vitro*. Pre-mRNA 3′-end processing assays with different yeast cell extracts *in vitro* (**A**) Cleavage reactions with *clp1* mutant extracts. Extracts from wild-type (lane 2, 3 and 9) or *clp1* mutant strains (lanes 4–8, 10, 15–18) were tested under standard cleavage assay conditions with *CYC1* pre-mRNA (lane 1, unreacted precursor). Efficient complementation of the deficient extracts prepared from the Ts alleles (lane 12, 13, 14 and 18) was obtained with 0,5 µl of purified CF IA, otherwise inactive on its own (lane 11). However, recombinant Clp1p poorly complemented the Ts mutant extracts (lanes 16, 17). WT, extracts prepared from the wild-type strain BMA64 (31); *CLP1*, extracts prepared from YLM176 (lane 2) or YLM127 (lane 9; see Supplementary Table S1). (**B**) Specific polyadenylation assays with wild-type, *clp1-5* and *clp1-12* Ts mutant extracts on the pre-cleaved *CYC1* precursor RNA (lane 1, unreacted *CYC1*pre). Low complementation of the deficient extracts was observed with 30 ng of recombinant protein Clp1p (lanes 4 and 7), whereas complete restoration was obtained with purified CF IA (lanes 5 and 8). Positions of the polyadenylated, 5′- or 3′-cleaved products are indicated; M, molecular weight markers in number of nucleotides.

destabilizing cassette consisting of a ubiquitin–arginine moiety fused at the N-terminus of the protein of interest (36,46). The efficient depletion was confirmed by western blot analysis of extracts prepared from cells grown in galactose only (GAL), or from cells grown in galactose and then shifted for 4 h to a glucose-containing medium (GLU) (Figure 3B). In glucose-shifted cells, ubiquitin-Arg-modified proteins were selectively depleted, whereas levels of the three other CF IA subunits were not affected (Figure 3B, lanes 2 and 4).

We next performed primer extension analysis of transcripts from the *SNR13-TRS31* region of the genome as described previously (36), using the same strains as above (Figure 3C). An oligonucleotide complementary to the *TRS31* ORF revealed extended transcripts by reverse transcription on total RNA extracted from the *GAL::(Arg)-CLP1* and *GAL::(Arg)-PCF11* strains after a shift to glucose (Figure 3D, lanes 3 and 6, product Y) but not from the same strains grown in galactose, or from the wild-type strain (Figure 3D, lanes 1, 2, 4, 5, and 7, 8, respectively; only product X is detected). For comparison, RNA extracted from the Ts *rna15-1* and *pti1-2* mutants shifted to 37°C were also tested and showed a defect in *SNR13* 3′-end formation, as previously demonstrated (36,45). In this experiment, extended product Y corresponds to a transcription termination defect at the 3′ end of Box C/D snoRNA *SNR13*, correlating with deficient snoRNA 3′-end formation. Several other snoRNAs, of

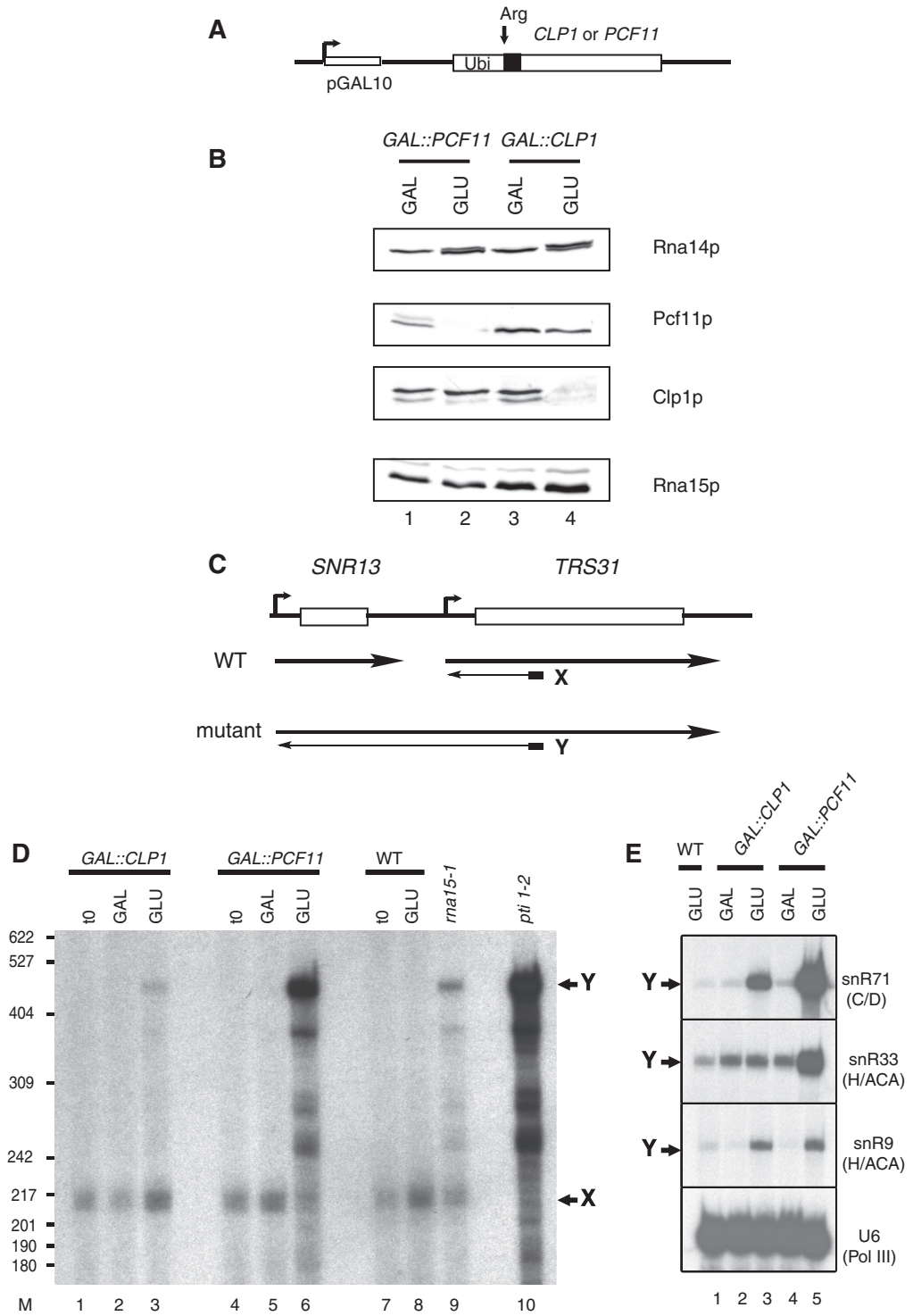

Figure 3. snoRNA 3′-end formation in Clp1p- and Pcf11p-depleted cells. Processing at the 3′-ends of snoRNA transcripts is tested by primer extension analysis. (**A**) Schematic representation of conditional alleles *GAL::(Arg)-CLP1* and *GAL::(Arg)-PCF11*. Expression of Ubiquitin-R-Clp1p or Ubiquitin-R-Pcf11p fusion proteins is driven by the inducible *GAL* promoter. After de-ubiquitylation *in vivo*, the unstable proteins R-Clp1p or R-Pcf11p are readily degraded, according to the N-end rule pathway (60). (**B**) Immunoblot analysis of extracts (40 µg) prepared from *GAL::CLP1* or *GAL::PCF11* cells grown in galactose medium (GAL) or after a 4 h-shift to glucose (GLU). The blots were probed with antibodies to Rna14p (1:3000), Pcf11p (1:2000), Clp1p (1:1000) or Rna15p (1:10 000). (**C**) Schematic illustration of the *SNR13-TRS31* chromosomal locus. Reverse transcription analysis was carried out with a probe complementary to the coding strand of *TRS31* ORF. 'X' refers to reverse transcription products found in normal conditions while product 'Y' reveals snR13 readthrough transcripts. (**D**) Polyacrylamide gel electrophoresis of reverse transcripts of snR13. Reverse transcription was performed on RNAs extracted from *rna15-1* and *pti1-2* strains after a shift to 37°C for 2 h (lanes 9–10), or from *GAL::CLP1* and *GAL::PCF11* cells grown in galactose medium ($t = 0$), and after their transfer to galactose (GAL) or glucose (GLU) medium for 4 hours (lanes 2–3 and 5–6, respectively). Lanes 7–8, reverse transcription analysis of RNAs from a wild-type control shifted from galactose to glucose as above. M, molecular weight markers in number of nucleotides. (**E**) Reverse transcription analysis of several box C/D and H/ACA snoRNAs from wild-type, *GAL::CLP1* and *GAL::PCF11* cells grown in galactose (GAL) or glucose (GLU) medium, as in (D). Extended product 'Y' is shown only. The pol III-transcribed U6 RNA is given as a normalization control for the reverse transcription.

both box C/D and H/ACA classes, were also affected by depletion of Clp1p and Pcf11p (Figure 3E). As we could observe, each tested snoRNA transcription unit was not affected to the same extent by depletion of Clp1p and Pcf11p. In particular, snR9 was equivalently affected by depletion of both proteins, and equal readthrough products accumulated with snR33 when Clp1p was either overexpressed or depleted. We are currently unable to explain these differences, but our results reflect the importance of Clp1p in transcription termination at snoRNA genes. As a result, we conclude that the whole CF IA complex participates in 3′-end formation of independently transcribed snoRNA genes in yeast.

Ts *clp1* alleles impinge on CF IA organization

To extend our analysis of the effect of *CLP1* gene mutations, we purified CF IA in the different mutant backgrounds depicted in Figure 1 (see Supplementary Table S1 for their genotypes). We generated *clp1* mutant strains in which *RNA15* was TAP-tagged. Except for the Ts strains, purified CF IA exhibited a subunit composition similar to wild-type (Figure 4A, upper panel, compare lanes 2, 3, 9 to lane 1). In addition, careful examination of CF IA purified from the temperature-resistant *clp1-17* mutant (G335S/L341S) showed normal levels of Rna14p and Rna15p, but lower amounts of both Clp1p and Pcf11p (Figure 4A, lane 7). Although only Clp1p is mutated, the amount of Clp1p and Pcf11p displayed a similar decrease. CF IA purified from the Ts mutant alleles (*clp1-5, -15, -16*) were completely devoid of Clp1p but more surprisingly of Pcf11p as well (Figure 4A, lanes 4–6). The relative amounts of Clp1p, Pcf11p and Rna15p were detected by western blots from equal amounts of purified factors probed with antibodies against these proteins (Figure 4A, lower panel).

Multiple interactions between CF I and CPF have been reported (10,16,21,47–49). To determine whether *clp1* Ts mutations also disrupted interactions with CPF subunits, we purified the whole [CF IA+CPF] complex in strains where both *RNA15* and *FIP1* (subunit of CPF) were TAP-tagged. In all the *clp1* Ts mutants analysed, the band pattern of CPF proteins were similar to the wild-type factor (Figure 4B, silver stained gel). Specifically, the four largest subunits corresponding to the CF II sub-complex of CPF [Cft1p/Yhh1p, Cft2p/Ydh1p, Ysh1p/Brr5p and Pta1p; (50)] were all clearly visible, as well as poly(A) polymerase Pap1p and Pfs2p. Although no Clp1p could be seen in [CF IA+CPF] purified from either *clp1-5* or *clp1-15*, a faint band migrating at the same size as Pcf11p in wild-type factors was discernible in the *clp1-5* mutant but not in the *clp1-15* complex (Figure 4B, lanes 3, 4). Western blot analysis with specific antibodies confirmed the presence of CF IA subunits and Pap1p (Figure 4C). It is noticeable that the *clp1-5* allele is less affected by high temperature than the *clp1-15* or *clp1-12* alleles (Figure 1B and D). As a result, simultaneous purification of [CF IA+CPF] could force the cohesion of the two factors and may explain why a residual amount of Pcf11p was co-purified in the less affected *clp1-5* allele. However, when CF IA was purified alone from *RNA15* TAP-tagged strain, Pcf11p was neither observed in *clp1-5* nor in *clp1-15* or *clp1-16* (Figure 4A), since partitioning of CF IA and CPF may have been forced by the purification procedure. Specific antibodies to Ref2p, Mpe1p and Pti1p revealed similar amounts of these polypeptides in [CF IA+CPF] purified from either the wild-type or *clp1-15* strains (Figure 4E).

To complement the analysis of the purified factors, we tested their ability to cleave *CYC1* and polyadenylate *CYC1* pre-cleaved precursors in assays similar to those performed with extracts (reported in Figure 2). Consistently, [CF IA+CPF] purified from the Ts mutants were unable to cleave or polyadenylate the *CYC1* precursors (Supplementary Figure S2).

These results indicate that association of Clp1p and Rna14p/Rna15p around Pcf11p is dependent upon Clp1p and that this organization is required for the function of CF IA in 3′-end formation.

Clp1p fails to interact with Pcf11p in the *clp1* Ts mutants

Purification of CF IA in the different *clp1* Ts mutants showed that both Clp1p and Pcf11p could not associate with Rna14p/Rna15p. However, Rna14p and Rna15p were still able to interact with each other. We wondered whether Pcf11p was still able to interact with the mutant Clp1 proteins. We co-expressed the different alleles of *CLP1* in *E. coli* (diagrammed in Figure 1C) together with the histidine-tagged Clp1p-binding region of Pcf11p (amino acids 454–563) (26). Pull-down experiments demonstrated that all of the proteins encoded by the temperature-resistant alleles (*clp1-1, -6, -13, -17, -19*) were able to interact with His_6-tagged $Pcf11p^{(454–563)}$. However, none of the Ts mutant polypeptides (*clp1-5, -15, -16*) co-precipitated with $Pcf11p^{(454–563)}$ (Figure 5A). Western blot analysis of total *E. coli* extracts expressing the various constructs with anti-Clp1p antibodies showed that the wild-type and mutant proteins were all expressed, confirming that the loss of interaction with $Pcf11p^{(454–563)}$ correlated with the Ts mutations and was not due to the absence of protein expression or instability (Figure 5B). It is interesting to observe on the western blot that the various forms of Clp1p displayed different migration behaviours. Proteins encoded by *clp1-13, -15,-16, -17,* and *clp1-19* alleles migrated with apparent molecular weight slightly larger than the other alleles (Figure 5B, compare the Clp1 proteins on lanes 7–11 to lanes 3–6 of the western blot). We found no direct correlation between the migration pattern and the temperature-sensitivity of the encoded proteins; however, a link potentially exists with the presence of the L341S mutation, either alone (Clp1-19p; see Figure 1C) or associated with one or two other mutations (Clp1-15p, -13p, -16p, and -19p). Currently, this observation has not been investigated further but may arise from unknown protein modification and/or abnormal migration properties of these proteins in SDS gels.

Finally, we tested the ability of Clp1p and its mutant versions to interact with full-length Pcf11p with the 2-hybrid method using *HIS3* as reporter gene (51,52). To counteract some leakiness of the system, 5 mM of

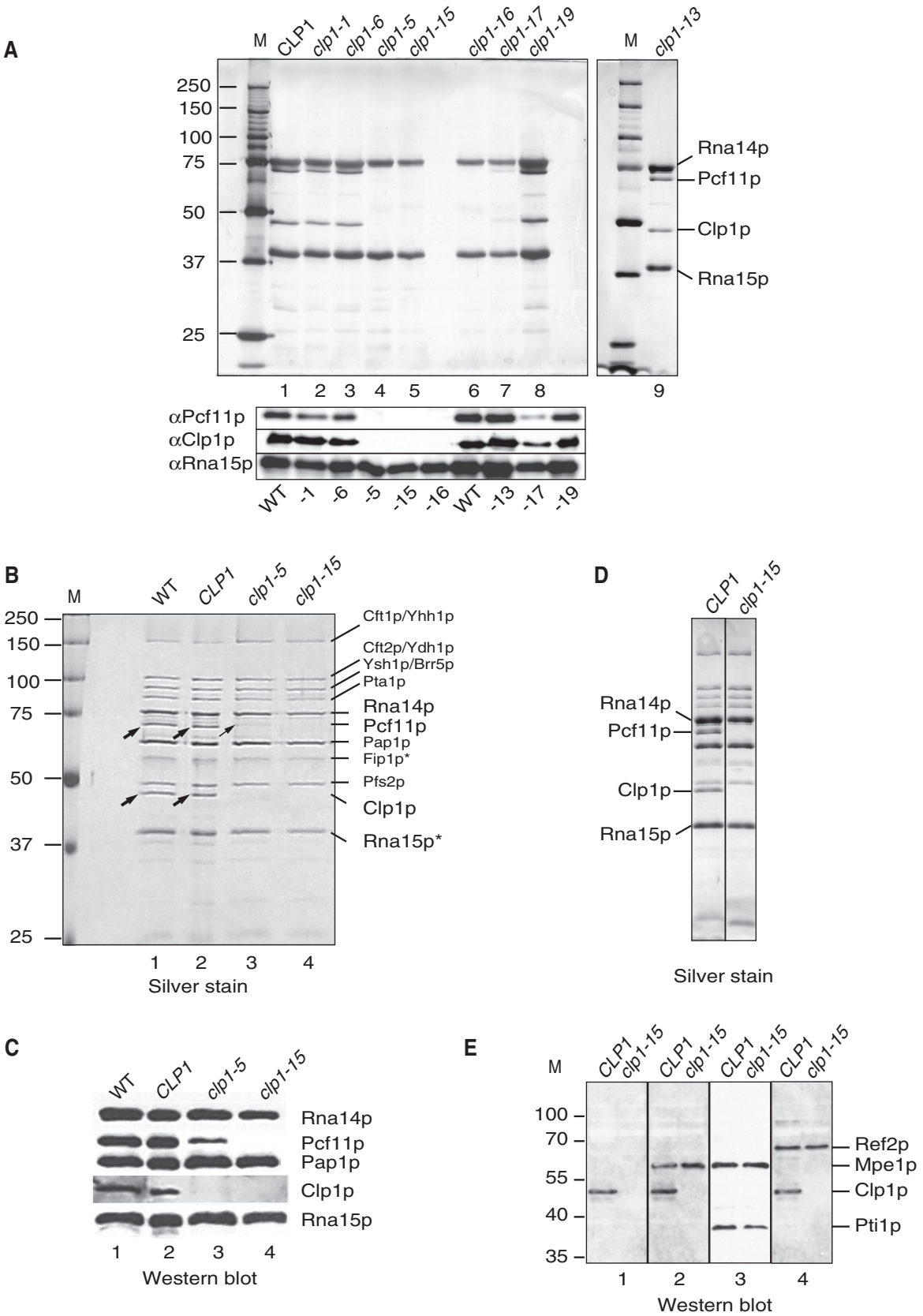

Figure 4. Architecture of CF IA is destabilized by Ts mutations in the *CLP1* gene. Purification of 3′-end processing complexes from wild-type and *clp1* mutant strains. (**A**) TAP-tagged Rna15p was used to purify CF IA from the different *clp1* mutants as indicated on the top of the figure. The different *CLP1* alleles are borne on plasmids (see Supplementary Table S1). Purified complexes were run on 10% polyacrylamide–SDS gels and stained with silver. Lower panels: equivalent amounts of factors were immunoblotted with antibodies to Pcf11p, Clp1p and Rna15p, to attest for the

(continued)

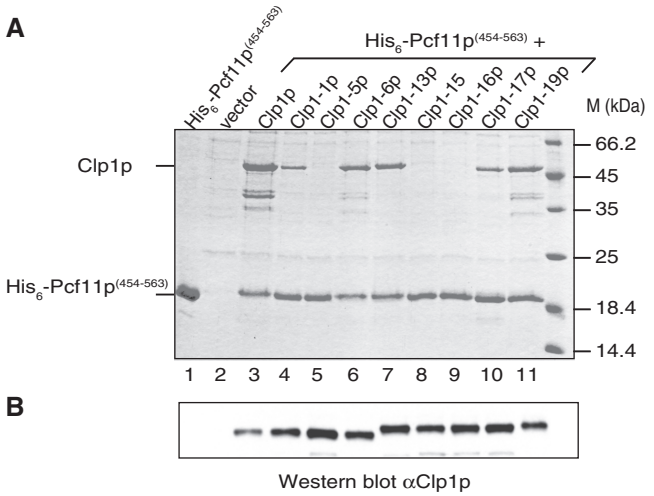

Figure 5. Pcf11p can no longer interact with Ts forms of Clp1p. Pull-down experiments with His_6-$Pcf11p^{(454–563)}$ and the different alleles of Clp1p co-expressed in *E. coli*. (**A**) The proteins were co-expressed in BL21(DE3) cells and pulled down with a cobalt-affinity resin. The bound proteins were released by boiling in loading buffer, run on a 15% polyacrylamide–SDS gel and stained with Coomassie. Lane 1, expression of His_6-$Pcf11p^{(454–563)}$ alone in bacteria; lane 2, control with expression vector alone; lanes 3-11, co-expression of His_6-$Pcf11p^{(454–563)}$ with all the different forms of Clp1p, as diagrammed in Figure 1A and C. M, molecular weight makers, in kiloDaltons. (**B**) Aliquots of supernatants from the pull-down assays were loaded on a 10% polyacrylamide–SDS gel and immuno-blotted with antibodies to Clp1p to attest for the expression of the different versions of the protein. Loading was done in the same order as in (A). Interaction between Clp1 mutant proteins and full-length Pcf11p were also tested with the 2-hybrid system *in vivo* (see Supplementary Table S2).

3-amino-1,2,4-triazole (3-AT) was added to inhibit residual growth on media lacking histidine even in the absence of interacting proteins. Therefore, cells carrying the empty pACT3 vector can no longer grow at any temperature tested in the presence of 3-AT (Supplementary Table S2, lane pACT3). Pcf11p is fused to the Gal4p DNA-binding domain to form the bait, and different alleles of *CLP1* were merged to the activating domain of *GAL4* to make the prey. We observed that both the WT and *clp1-1* temperature-resistant alleles could grow on medium lacking histidine supplemented with 3-AT. However, the three Ts alleles tested (*clp1-5, -15* and *-12*) were unable to grow at 37°C, and even at 30°C for *clp1-12* (Supplementary Table S2). These results confirm that the Clp1 proteins encoded by the Ts alleles fail to interact with wild-type full-length Pcf11p *in vivo*.

Recruitment of CF IA subunits to the 3′-end of a protein-coding gene in the *clp1-15* mutant

Rna14p, Rna15p and Pcf11p subunits of CF IA have been shown to associate strongly with the transcription elongation complex (EC) *in vivo* near polyadenylation sites of protein-coding genes (41). This association relies on the ability of Pcf11p to directly interact with the Pol II CTD (23). To determine whether Ts mutations in the *CLP1* gene that affect CF IA assembly may also perturb their association with the chromatin, we performed ChIP with TAP-tagged polyadenylation factors. We first demonstrated that wild-type Clp1p was able to crosslink to the 3′-end region of the *ADH1* gene, as the other three CF IA subunits (Figure 6A). The predominant amplification of PCR fragment number 3 illustrated this preferred localization (Figure 6B and C). The enhanced occupancy of Clp1p observed when cells were shifted from 24°C to 37°C most likely reflects the average increase of transcription rates observable after a 1 h shift to 37°C, as reported previously (53). We then tested the ability of the mutant Clp1-15 protein to crosslink near the polyadenylation site. If Clp1-15p could still crosslink at the permissive temperature as efficiently as the wild-type protein, we observed that the signal is lost after shift to the non-permissive temperature (Figure 6B, right panels).

We next examined cross-linking of Pcf11p and Rna15p to the *ADH1* gene. In the wild-type *CLP1* strain, Pcf11p and Rna15p cross-linked strongly to the 3′ region of the *ADH1* gene at both 24°C and 37°C (Figure 6D and F, respectively). In the *clp1-15* mutant background, cross-linking of Pcf11p was moderately affected at 37°C in comparison to the crosslink measured at 24°C (Figure 6D and E). On the other hand, the Rna15p crosslink dropped by half in comparison to that observed at the permissive temperature (Figure 6F-G). This difference can be explain by the fact that Pcf11p bears an independent domain that specifically interacts with the CTD of RNA polymerase II (23). Hence, it may be less sensitive to mutations in the *CLP1* gene that Rna15p in the ChIP assay.

It has been shown recently that Rna14p and Rna15p are tightly associated with each other via their monkeytail and hinge domains, respectively, to such an extent that only mutations within one of these regions disrupt their association (19). As Rna14p still binds to Rna15p in the purified factor (Figure 4), we anticipate from the loss of Rna15p cross-link in the *clp1-15* mutant that association of Rna14p with the chromatin may also drop to the same extent. In a similar situation, *rna14-1* mutation abolished Rna15p cross-linking at the 3′-end of genes (41).

Figure 4. Continued
presence of the subunit. M, molecular weight makers, sizes in kDa are indicated on the left. (**B**) Co-purification of [CF IA+CPF] from wild-type and *clp1* Ts mutant strains where both Rna15p and Fip1p where TAP-tagged (the tagged subunit is marked with a asterisk). WT, wild-type factors prepared from YSD13 [lane 1; (38); *CLP1* (lane 2), *clp1-5* (lane 3), *clp1-15* (lane 4)]: factors prepared from strains where the different *CLP1* alleles are carried on a plasmid (see Supplementary Table S1). Protein complexes were run on 10% polyacrylamide–SDS gels and stained with silver, as in (B). Arrows point to the Pcf11 and Clp1 proteins. M, molecular weight makers, in kiloDaltons. (**C**) Purified [CF IA+CPF] shown in (B) were analysed by immunoblotting with antibodies to Rna14p, Pcf11p, Pap1p, Clp1p, and Rna15p to check for their presence. Equal amounts of [CF IA+CPF] purified from wild-type (YRH73) and mutant *clp1-15* (YRH69) strains were run on 10% polyacrylamide–SDS gels and either stained with silver (**D**), or (**E**) immunoblotted with antibodies against Clp1p (blot 1), Mpe1p and Clp1p (blot 2), Mpe1p and Pti1p (blot 3) and Ref2p and Clp1p (blot 4). *In vitro* 3′-end processing assays were also performed with the purified [CF IA+CPF] factors (see Supplementary Figure S2).

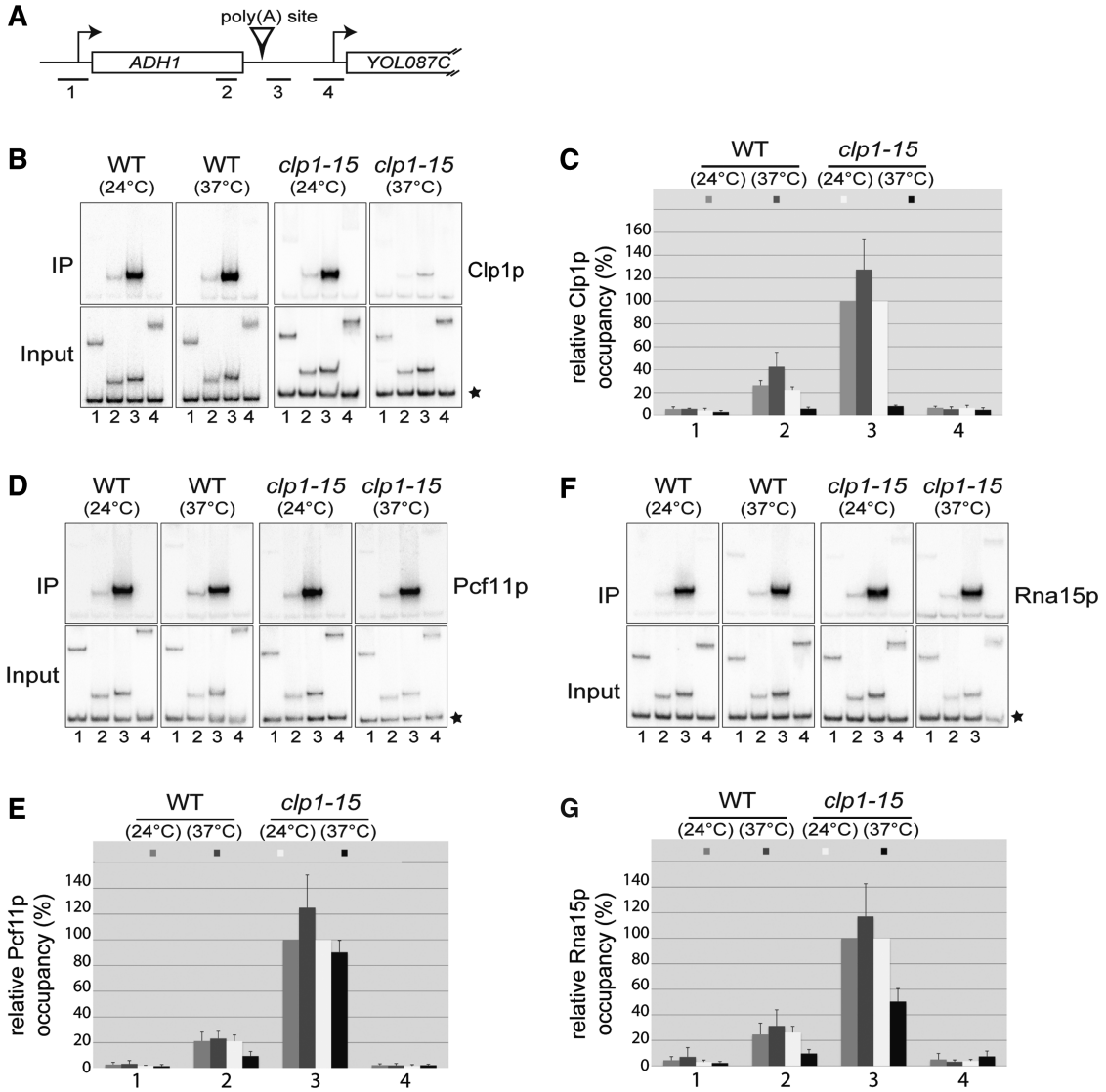

Figure 6. Cross-linking of CF IA subunits at the 3′-end of the *ADH1* gene. Strains carrying TAP-tagged Clp1p, Clp1-15p, Pcf11p, or Rna15p were analysed by ChIP of the *ADH1* gene. (**A**) Schematic representation of the *ADH1-YOL087C* locus on the chromosome. Broken arrows represent the transcription start sites, the open arrowhead shows the polyadenylation site. The four fragments amplified by PCR and used in the ChIP analysis are represented as bars below the gene and numbered. (**B**) ChIP analysis with TAP-tagged Clp1p-and TAP-tagged Clp1-15p-expressing strains cultivated at the permissive temperature (24°C) or shifted to 37°C for 1 h. PCR-amplified fragments of IP chromatin were analysed by electrophoresis on 8% non-denaturing polyacrylamide gels. IP, chromatin IP by TAP-tagged Clp1p and subjected to PCR with primer pairs amplifying fragments 1–4 as depicted in (A); Input, total input chromatin. Asterisk: background control from a non-transcribed region of chromosome V. (**C**) Clp1p and Clp1-15p occupancy values quantitated as described in 'Materials and Methods' section. The TAP-tagged Clp1p and Clp1-15p-expressing strains (YLM204 and YLM215, respectively) were grown at 24°C or shifted to 37°C for 1 h. For easier comparison, the highest value obtained with fragment number 3 for each immunoprecipitation was set up to 100 and other values were expressed relative to this maximum. Values represent the average of three independent experiments, and error bars indicate average deviations. (**D** and **E**) ChIP analysis with TAP-tagged Pcf11p in *CLP1* (WT; YLM198) and *clp1-15* (YLM201) strains cultivated at the permissive temperature (24°C) or shifted to 37°C for 1 h. Quantitation of results were carried out as in (C). **(F** and **G)** ChIP analysis on *ADH1* and quantitation of the results obtained with TAP-tagged Rna15p in *CLP1* (WT; YLM184) and *clp1-15* (YLM206) strains cultivated at 24°C and shifted to 37°C as in **(**D and E**)**. Values in (D and E**)** and **(**F and G**)** represent the average of three independent experiments, and error bars indicate average deviations.

Therefore, cross-linking of CF IA subunits to the 3′-end of genes is sensitive to mutations in the *CLP1* gene. The less efficient recruitment of Rna15p in *clp1-15* mutant and the overall destabilization of CF IA complex very likely influences negatively the efficiency of the coupling between transcription termination and 3′-end formation.

Altogether, the results presented in this article strongly suggest that Clp1p is required to maintain the assembly of a functional CF IA in order to ensure its function in pre-mRNA 3′-end processing and transcription termination.

DISCUSSION

In this study, we have investigated the function of the yeast Clp1 protein, one of the four subunits of CF IA,

factor involved in polyadenylation. We have isolated Ts mutants of the *CLP1* gene that abolish pre-mRNA 3′-end cleavage and polyadenylation and showed that *in vivo* depletion of Clp1p and Pcf11p inhibit termination of transcription at Pol II-transcribed snoRNA genes. Therefore, altered expression of all four subunits of CF IA abolish 3′ processing and transcription termination (1,20,23,24,37,42), underscoring the essential role of this factor in the coupling of polyadenylation and Pol II termination. Clp1 also exists in humans and exhibits an RNA-kinase activity in tRNA splicing, as a component of the tRNA splicing endonuclease complex, and in siRNA activation (28). Associated with hPcf11 in CF II_m, hClp1 is required for cleavage of the pre-mRNA transcript (25). However, its role as a kinase in pre-mRNA 3′-end processing has not been documented. The enzymatic activity of Clp1 was predicted by the presence of a P-loop/Walker A motif in its primary sequence, reinforced by the crystal structure of the yeast protein (26). Despite these particular features, no kinase activity has yet been ascribed to yeast Clp1p (26,27).

The mutations found to inhibit processing are located within the ATP-binding domain and the Clp1p–Pcf11p interacting region. The most striking feature of these mutations is that they have to be combined to cause temperature-sensitivity. Remarkably, this phenotype is always linked with dissociation of the tetrameric architecture of CF IA, leaving Rna14p/Rna15p together on one side whereas Pcf11p and Clp1p fall apart individually. Alternatively, combination of two mutations at the Clp1p-Pcf11p interface (G335S/L341S) did not result in the loss of interaction between both of them, nor result in a conditional lethal phenotype. Therefore, it seems likely that CF IA remains assembled and functional as long as Pcf11p can interact with Clp1p. Since Pcf11p is the only component of CF IA to interact with all of the other subunits, Clp1p may send a 'signal' through Pcf11p to allow the association of Rna14p/Rna15p. We propose that the interaction between Clp1p and Pcf11p involves conformational rearrangements of both proteins such that Rna14p/Rna15p associate with CF IA. Additionally, these conformational changes must rely on an intact ATP binding site. The G135R mutation we found in the P-loop domain has no phenotypic effect on yeast. Other mutants have been described in which the neighbouring amino acids K136-T137 were changed into alanine. These mutants are also viable with no detectable phenotype at 37°C (27). Yet, equivalent mutations in the P-loop domain of either hClp1 or the T4 polynucleotide kinase abolish their activity (27,28). We postulate that the G135R mutation in yeast Clp1p has no detectable effect on growth because it affects only moderately the conformational rearrangement of the protein, such that Pcf11p can still interact efficiently with Clp1p and thus recruit Rna14p/Rna15p. However, additional mutations, such as G335S or L341S, in the distant Clp1p–Pcf11p binding region (Supplementary Figure S1B), may modify the structure of Clp1p to such an extent that it can no longer interact with Pcf11p and induce the conformational change to Pcf11p required to recruit Rna14p/Rna15p. In the double mutant *clp1-17* (G335S/L341S), a decrease in the amount of both Clp1p and Pcf11p associated with purified CF IA does not result in a lethal phenotype. This reinforces the concept that the ATP-binding domain has an essential function, as mutations in it have a synergistic lethal effect at 37°C when combined with single mutations at the Clp1p-Pcf11p interface. Our data are showing that Pcf11p–Clp1p interaction is essential. Whether or not they can act *in vivo* as a dimer, as in mammals within CF II_m, adjacent to a dimeric Rna14p/Rna15p sub-complex, remains unknown but our mutants might cast light on the separation of mammalian CF II_m and CstF (comprising Rna14p/Rna15p counterparts) in evolution.

The potential change in the Clp1p ATP-binding pocket due to the G135R mutant can be predicted from the available crystal structure of Clp1p-Pcf11p$^{(454\text{-}563)}$ (26). In the wild-type protein, the G135 backbone amide provides hydrogen-bonding to the β-phosphate group of the ATP. This interaction is further stabilized by the adjacent amino acids T134, K136 and T137. The α- and γ-phosphates are also bound by residues of the Clp1p base-binding loop. The G135R mutation would be predicted to provoke perturbation of this extensive binding network due to the significantly larger side-chain of arginine compared to glycine (Figure 7). It is most likely that the arginine side chain interferes with the ATP binding and also its orientation in its binding pocket, although

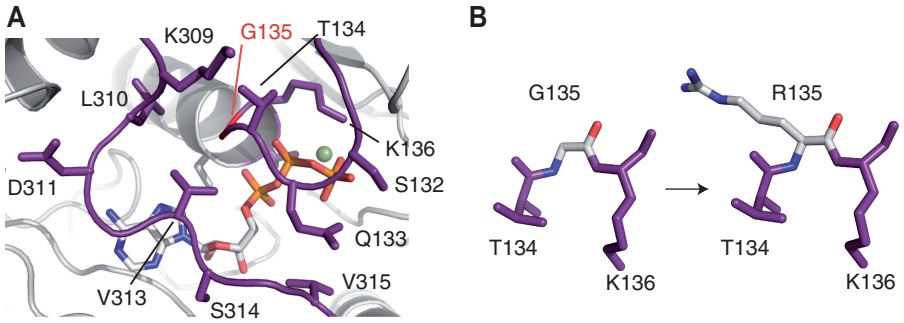

Figure 7. The Clp1p ATP-binding site. (**A**) Close view of the ATP-binding pocket of Clp1p, according to Noble *et al.* (26). Residues of the Switch I and II loops are shown in purple. The G135 position is coloured in red. The Mg^{2+} ion is coloured in green. (**B**) Cartoon representation of the G135R mutation and the neighbouring amino acids, emphasizing the side chain difference between the two amino acids.

an opposing stabilizing effect cannot be ruled out. In either case, the change of the ATP-binding region nevertheless remains non-lethal until an additional mutation is introduced in the quite remote Pcf11p-interaction domain. The combined effect effectively prevents, accentuates or otherwise alters the normal transduction of the conformational change such that the lethal phenotype results.

In addition to the effect of the *clp1* Ts mutations on the assembly of the purified factor, we have also investigated the consequence on the recruitment of CF IA subunits to the elongating Pol II on the chromatin. We have found that these mutations decrease slightly but significantly the cross-linking of Pcf11p to the *ADH1* polyadenylation site while they more severely affect Rna15p recruitment. The loss of Rna15p cross-linking is consistent with its separation from the purified factor together with Rna14p to which it interacts tightly, by way of their hinge and monkeytail domains, respectively (19). If we consider Pcf11p as the scaffolding subunit of CF IA around which Clp1p, Rna14p/Rna15p organize, we can envisage that recruitment of Rna14p/Rna15p to the chromatin previously reported (41) may only occur if Clp1p interacts productively with Pcf11p. The finding that Pcf11p is still able to partially crosslink near the poly(A) site in *clp1* mutants may likely be due to the fact that Clp1p, Rna14p, and Rna15p-interacting regions of the protein are not overlapping with its CID (23). Therefore, the assumption that mutant Clp1 proteins can no longer induce conformational changes through Pcf11p does not necessarily imply that it impinges on the direct interaction between Pcf11p and Pol II CTD.

It is well established that termination of transcription by RNA polymerase II is dependent upon both the 3′-end processing signals and the cleavage/polyadenylation factors (1,23,24,41,54). In *clp1* mutants, Pcf11p is still recruited to the 3′-end of genes and does not crosslink beyond the site of termination since fragment 4 does not co-immunoprecipitate with Pcf11p (Figure 6). It has been shown by Gilmour and colleagues (55) that the CID of yeast Pcf11p is able to dismantle *in vitro* Pol II ECs, thus triggering transcription termination. Their conclusions have been extended to dPcf11 in *Drosophila* (56). They propose that CF IA first recognizes the positioning element of the polyadenylation signal after synthesis, allowing subsequent Pcf11p recruitment to Pol II CTD. In this configuration, Pcf11p can bridge both the CTD and the transcript, creating forces that are transmitted to the EC, resulting in the dissolution of the complex and termination (55). Conformational changes are invoked to induce CTD rearrangements so that the RNA can no longer interact with Pcf11p CID.

We believe our results are compatible with this model and extend it further. We observed that Clp1p binding to Pcf11p is required to allow formation of a stable tetrameric factor. In the normal situation *in vivo*, CF IA binds to the nascent transcript emerging from the elongating polymerase, permitting the interaction of Pcf11p with Pol II-CTD. We postulate that the conformational changes of the CTD proposed by Zhang *et al.* (55) and required to dismantle Pol II EC would be transmitted through Pcf11p by Clp1p *in vivo*. This mechanism would maintain the obligatory association of CF IA-bound primary transcript and the EC to allow efficient dismantling. This cascade of conformational changes, transmitted to the CTD and the nascent transcript, could involve ATP hydrolysis by the putative kinase activity of Clp1p, only in the context of the whole machinery. This enzymatic activity is not observable *in vitro* with recombinant Clp1p (26) or even with Clp1p embedded in CF IA (L.M.-S., unpublished observation). In this model, conformational changes after ATP hydrolysis would be triggered by the interaction of Clp1p/CF IA with other components of the processing complex. Clp1p is structurally related to members of the SIMIBI class of ATPases (26,57), such as the *Azobacter vinelandii* NifH nitrogenase and the *E. coli* detoxification pump protein ArsA. These proteins are subunits of macromolecular complexes and nucleotide hydrolysis is activated only upon their interaction with members of the complex. Interestingly, ATP hydrolysis is required to induce conformational rearrangements (58,59). These data on related proteins of the same family with ATPase activity support our model that Clp1p may have kinase activity required during 3′-end processing-coupled transcription termination.

The fact that Pcf11p is capable of dismantling the EC as reported by Zhang *et al.* (55) without the help of Clp1p or any additional external activity might be due to the fact that these experiments were carried out *in vitro* in a simplified system where isolated ECs and Pcf11p CID were used. In this situation, it may be that the CID is constitutively active with regard to termination by dismantling of the Pol II EC.

In the *clp1* Ts mutant situation, CF IA disassembles after the shift to the non-permissive temperature and cleavage of the primary transcript is abolished. Pcf11p can still interact with Pol II CTD via its independent CID but Clp1p-induced conformational changes can no longer be transmitted through components of the polyadenylation machinery and termination does not occur.

In agreement with our results, C. Moore and coworkers (Ghazy *et al.*, accepted for publication) found that drastic amino acid changes in the ATP-binding site, K136E and T137W, are lethal. They propose that these mutations modify the orientation of the ATP molecule within its pocket to such a point that it blocks Clp1p in a non-reversible conformation. Consistently, the mutant proteins can no longer interact with Pcf11p. They also show that mutations in Pcf11p that disrupt Clp1/Pcf11p interaction have the same dramatic effects on 3′ processing and transcription termination that we found in our study.

Further experiments will be required to test the validity of this model. For instance, it would be important to show that CF IA is indeed capable *in vitro* of dismantling the elongating polymerase complex as does Pcf11p CID alone. In the case of a mutant Clp1p that does not provoke dissociation of the factor but affects its putative catalytic activity, one might also see that EC dismantling is affected. This *in vitro* system could possibly reveal the yet mysterious kinase activity of yeast Clp1p.

SUPPLEMENTARY DATA

Supplementary Data are available at NAR Online: Supplementary Tables S1–S2, Supplementary Figures S1–S2, Supplementary reference (51).

ACKNOWLEDGEMENTS

The authors gratefully acknowledge Dr Cameron Mackereth and Dr Derek McCusker for critical reading of the article; Chiara Pascali, Domenico Libri, Mathieu Rougemaille and Laurent Kuras for their advice on ChIP experiments, Cécile Monfoulet for technical assistance and Hélène Dumay-Odelot, Cameron Mackereth and Derek McCusker for fruitful discussions.

FUNDING

Centre National de la Recherche Scientifique; the French Ministère de la Recherche Scientifique; La Fondation pour la Recherche Médicale/Fondation BNP-Paribas (to L.M.-S.); Pre-doctoral fellowship from the French Ministère de la Recherche et de la Technologie (to R.H., N.V.); post-doctoral fellowship from La Fondation pour la Recherche Médicale (to F.M.). Funding for open access charge: INSERM.

Conflict of interest statement. None declared.

REFERENCES

1. Birse,C.E., Minvielle-Sebastia,L., Lee,B.A., Keller,W. and Proudfoot,N.J. (1998) Coupling termination of transcription to messenger RNA maturation in yeast. *Science*, **280**, 298–301.
2. Greger,I.H. and Proudfoot,N.J. (1998) Poly(A) signals control both transcriptional termination and initiation between the tandem *GAL10* and *GAL7* genes of *Saccharomyces cerevisiae*. *EMBO J.*, **17**, 4771–4779.
3. Kim,M., Krogan,N.J., Vasiljeva,L., Rando,O.J., Nedea,E., Greenblatt,J.F. and Buratowski,S. (2004) The yeast Rat1 exonuclease promotes transcription termination by RNA polymerase II. *Nature*, **432**, 517–522.
4. Teixeira,A., Tahiri-Alaoui,A., West,S., Thomas,B., Ramadass,A., Martianov,I., Dye,M., James,W., Proudfoot,N.J. and Akoulitchev,A. (2004) Autocatalytic RNA cleavage in the human beta-globin pre-mRNA promotes transcription termination. *Nature*, **432**, 526–530.
5. West,S., Gromak,N. and Proudfoot,N.J. (2004) Human 5′ –> 3′ exonuclease Xrn2 promotes transcription termination at co-transcriptional cleavage sites. *Nature*, **432**, 522–525.
6. Mandel,C.R., Bai,Y. and Tong,L. (2008) Protein factors in pre-mRNA 3′-end processing. *Cell Mol. Life Sci.*, **65**, 1099–1122.
7. Millevoi,S. and Vagner,S. (2010) Molecular mechanisms of eukaryotic pre-mRNA 3′ end processing regulation. *Nucleic Acids Res.*, **38**, 2757–2774.
8. Shi,Y., Di Giammartino,D.C., Taylor,D., Sarkeshik,A., Rice,W.J., Yates,J.R. 3rd, Frank,J. and Manley,J.L. (2009) Molecular architecture of the human pre-mRNA 3′ processing complex. *Mol. Cell*, **33**, 365–376.
9. Kessler,M.M., Zhao,J. and Moore,C.L. (1996) Purification of the *Saccharomyces cerevisiae* cleavage/polyadenylation factor I. *J. Biol. Chem.*, **271**, 27167–27175.
10. Minvielle-Sebastia,L., Preker,P.J., Wiederkehr,T., Strahm,Y. and Keller,W. (1997) The major yeast poly(A)-binding protein is associated with cleavage factor IA and functions in pre-messenger RNA 3′-end formation. *Proc. Natl Acad. Sci. USA*, **94**, 7897–7902.
11. He,X., Khan,A.U., Cheng,H., Pappas,D.L. Jr, Hampsey,M. and Moore,C.L. (2003) Functional interactions between the transcription and mRNA 3′ end processing machineries mediated by Ssu72 and Sub1. *Genes Dev.*, **17**, 1030–1042.
12. Gavin,A.C., Bosche,M., Krause,R., Grandi,P., Marzioch,M., Bauer,A., Schultz,J., Rick,J.M., Michon,A.M., Cruciat,C.M. *et al.* (2002) Functional organization of the yeast proteome by systematic analysis of protein complexes. *Nature*, **415**, 141–147.
13. Dichtl,B., Blank,D., Ohnacker,M., Friedlein,A., Roeder,D., Langen,H. and Keller,W. (2002) A Role for SSU72 in Balancing RNA Polymerase II Transcription Elongation and Termination. *Mol. Cell*, **10**, 1139–1150.
14. Kessler,M.M., Henry,M.F., Shen,E., Zhao,J., Gross,S., Silver,P.A. and Moore,C.L. (1997) Hrp1, a sequence-specific RNA-binding protein that shuttles between the nucleus and the cytoplasm, is required for mRNA 3′-end formation in yeast. *Genes Dev.*, **11**, 2545–2556.
15. Minvielle-Sebastia,L., Beyer,K., Krecic,A.M., Hector,R.E., Swanson,M.S. and Keller,W. (1998) Control of cleavage site selection during mRNA 3′-end formation by a yeast hnRNP. *EMBO J.*, **17**, 7454–7468.
16. Amrani,N., Minet,M., Le Gouar,M., Lacroute,F. and Wyers,F. (1997) Yeast Pab1 interacts with Rna15 and participates in the control of the poly(A) tail length *in vitro*. *Mol. Cell. Biol.*, **17**, 3694–3701.
17. Viphakone,N., Voisinet-Hakil,F. and Minvielle-Sebastia,L. (2008) Molecular dissection of mRNA poly(A) tail length control in yeast. *Nucleic Acids Res.*, **36**, 2418–2433.
18. Dunn,E.F., Hammell,C.M., Hodge,C.A. and Cole,C.N. (2005) Yeast poly(A)-binding protein, Pab1, and PAN, a poly(A) nuclease complex recruited by Pab1, connect mRNA biogenesis to export. *Genes Dev.*, **19**, 90–103.
19. Moreno Morcillo,M., Minvielle-Sébastia,L., Fribourg,S. and Mackereth,C.D. (2011) Locked tether formation by co-operative folding of Rna14p monkeytail and Rna15p hinge domains in the yeast CF IA complex. *Structure*, **19**, 534–545.
20. Amrani,N., Minet,M., Wyers,F., Dufour,M.-E., Aggerbeck,L.P. and Lacroute,F. (1997) *PCF11* encodes a third protein component of the yeast cleavage and polyadenylation factor I. *Mol. Cell. Biol.*, **17**, 1102–1109.
21. Gross,S. and Moore,C. (2001) Five subunits are required for reconstitution of the cleavage and polyadenylation activities of *Saccharomyces cerevisiae* cleavage factor I. *Proc. Natl Acad. Sci. USA*, **98**, 6080–6085.
22. Leeper,T.C., Qu,X., Lu,C., Moore,C. and Varani,G. (2010) Novel protein-protein contacts facilitate mRNA 3′-processing signal recognition by Rna15 and Hrp1. *J. Mol. Biol.*, **401**, 334–349.
23. Sadowski,M., Dichtl,B., Hubner,W. and Keller,W. (2003) Independent functions of yeast Pcf11p in pre-mRNA 3′ end processing and in transcription termination. *EMBO J.*, **22**, 2167–2177.
24. Barillà,D., Lee,B.A. and Proudfoot,N.J. (2001) Cleavage/polyadenylation factor IA associates with the carboxyl-terminal domain of RNA polymerase II in *Saccharomyces cerevisiae*. *Proc. Natl Acad. Sci. USA*, **98**, 445–450.
25. de Vries,H., Ruegsegger,U., Hubner,W., Friedlein,A., Langen,H. and Keller,W. (2000) Human pre-mRNA cleavage factor II(m) contains homologs of yeast proteins and bridges two other cleavage factors. *EMBO J.*, **19**, 5895–5904.
26. Noble,C.G., Beuth,B. and Taylor,I.A. (2007) Structure of a nucleotide-bound Clp1-Pcf11 polyadenylation factor. *Nucleic Acids Res.*, **35**, 87–99.
27. Ramirez,A., Shuman,S. and Schwer,B. (2008) Human RNA 5′-kinase (hClp1) can function as a tRNA splicing enzyme in vivo. *RNA*, **14**, 1737–1745.
28. Weitzer,S. and Martinez,J. (2007) The human RNA kinase hClp1 is active on 3′ transfer RNA exons and short interfering RNAs. *Nature*, **447**, 222–226.
29. Jain,R. and Shuman,S. (2009) Characterization of a thermostable archaeal polynucleotide kinase homologous to human Clp1. *RNA*, **15**, 923–931.
30. Greer,C.L., Peebles,C.L., Gegenheimer,P. and Abelson,J. (1983) Mechanism of action of a yeast RNA ligase in tRNA splicing. *Cell*, **32**, 537–546.

31. Baudin-Baillieu,A., Guillemet,E., Cullin,C. and Lacroute,F. (1997) Construction of a yeast strain deleted for the TRP1 promoter and coding region that enhances the efficiency of the polymerase chain reaction- disruption method. *Yeast*, **13**, 353–356.
32. Bonneaud,N., Ozier-Kalogeropoulos,O., Li,G., Labouesse,M., Minvielle-Sebastia,L. and Lacroute,F. (1991) A family of low and high copy replicative, integrative and single-stranded *S. cerevisiae*/*E. coli* shuttle vectors. *Yeast*, **7**, 609–615.
33. Stotz,A. and Linder,P. (1990) The *ADE2* gene from *Saccharomyces cerevisiae*: sequence and new vectors. *Gene*, **95**, 91–98.
34. Baudin,A., Ozier-Kalogeropoulos,O., Denouel,A., Lacroute,F. and Cullin,C. (1993) A simple and efficient method for direct gene deletion in *Saccharomyces cerevisiae*. *Nucleic Acids Res.*, **21**, 3329–3330.
35. Sikorski,R.S. and Boeke,J.D. (1991) In vitro mutagenesis and plasmid shuffling: from cloned gene to mutant yeast. *Methods Enzymol.*, **194**, 302–318.
36. Dheur,S., Vo,L.T.A., Voisinet-Hakil,F., Minet,M., Schmitter,J.M., Lacroute,F., Wyers,F. and Minvielle-Sebastia,L. (2003) Pti1p and Ref2p found in association with the mRNA 3′ end formation complex direct snoRNA maturation. *EMBO J.*, **22**, 2831–2840.
37. Minvielle-Sebastia,L., Preker,P.J. and Keller,W. (1994) RNA14 and RNA15 proteins as components of a yeast pre-mRNA 3′-end processing factor. *Science*, **266**, 1702–1705.
38. Dheur,S., Nykamp,K.R., Viphakone,N., Swanson,M.S. and Minvielle-Sebastia,L. (2005) Yeast mRNA Poly(A) tail length control can be reconstituted in vitro in the absence of Pab1p-dependent Poly(A) nuclease activity. *J. Biol. Chem.*, **280**, 24532–24538.
39. Lefevre,S., Dumay-Odelot,H., El-Ayoubi,L., Budd,A., Legrand,P., Pinaud,N., Teichmann,M. and Fribourg,S. (2011) Structure-function analysis of hRPC62 provides insights into RNA polymerase III transcription initiation. *Nat. Struct. Mol. Biol.*, **18**, 352–358.
40. Keogh,M.C. and Buratowski,S. (2004) Using chromatin immunoprecipitation to map cotranscriptional mRNA processing in *Saccharomyces cerevisiae*. *Methods Mol. Biol.*, **257**, 1–16.
41. Kim,M., Ahn,S.H., Krogan,N.J., Greenblatt,J.F. and Buratowski,S. (2004) Transitions in RNA polymerase II elongation complexes at the 3′ ends of genes. *EMBO J.*, **23**, 354–364.
42. Kim,M., Vasiljeva,L., Rando,O.J., Zhelkovsky,A., Moore,C. and Buratowski,S. (2006) Distinct pathways for snoRNA and mRNA termination. *Mol. Cell*, **24**, 723–734.
43. Walker,J.E., Saraste,M., Runswick,M.J. and Gay,N.J. (1982) Distantly related sequences in the alpha- and beta-subunits of ATP synthase, myosin, kinases and other ATP-requiring enzymes and a common nucleotide binding fold. *EMBO J.*, **1**, 945–951.
44. Fatica,A., Morlando,M. and Bozzoni,I. (2000) Yeast snoRNA accumulation relies on a cleavage-dependent/polyadenylation-independent 3′-processing apparatus. *EMBO J.*, **19**, 6218–6229.
45. Morlando,M., Greco,P., Dichtl,B., Fatica,A., Keller,W. and Bozzoni,I. (2002) Functional analysis of yeast snoRNA and snRNA 3′-end formation mediated by uncoupling of cleavage and polyadenylation. *Mol. Cell. Biol.*, **22**, 1379–1389.
46. Varshavsky,A. (1996) The N-end rule: functions, mysteries, uses. *Proc. Natl Acad. Sci. USA*, **93**, 12142–12149.
47. Kyburz,A., Sadowski,M., Dichtl,B. and Keller,W. (2003) The role of the yeast cleavage and polyadenylation factor subunit Ydh1p/Cft2p in pre-mRNA 3′-end formation. *Nucleic Acids Res.*, **31**, 3936–3945.
48. Ohnacker,M., Barabino,S.M., Preker,P.J. and Keller,W. (2000) The WD-repeat protein Pfs2p bridges two essential factors within the yeast pre-mRNA 3′-end-processing complex. *EMBO J.*, **19**, 37–47.
49. Preker,P.J., Lingner,J., Minvielle-Sebastia,L. and Keller,W. (1995) The *FIP1* gene encodes a component of a yeast pre-mRNA polyadenylation factor that directly interacts with poly(A) polymerase. *Cell*, **81**, 379–389.
50. Zhao,J., Kessler,M., Helmling,S., O'Connor,J.P. and Moore,C. (1999) Pta1, a component of yeast CF II, is required for both cleavage and poly(A) addition of mRNA precursor. *Mol. Cell. Biol.*, **19**, 7733–7740.
51. Fromont-Racine,M., Rain,J.C. and Legrain,P. (1997) Toward a functional analysis of the yeast genome through exhaustive two-hybrid screens. *Nat Genet*, **16**, 277–282.
52. Fromont-Racine,M., Rain,J.C. and Legrain,P. (2002) Building protein-protein networks by two-hybrid mating strategy. *Methods Enzymol.*, **350**, 513–524.
53. Gasch,A.P., Spellman,P.T., Kao,C.M., Carmel-Harel,O., Eisen,M.B., Storz,G., Botstein,D. and Brown,P.O. (2000) Genomic expression programs in the response of yeast cells to environmental changes. *Mol. Biol. Cell*, **11**, 4241–4257.
54. Bauren,G., Belikov,S. and Wieslander,L. (1998) Transcriptional termination in the Balbiani ring 1 gene is closely coupled to 3′-end formation and excision of the 3′-terminal intron. *Genes Dev.*, **12**, 2759–2769.
55. Zhang,Z., Fu,J. and Gilmour,D.S. (2005) CTD-dependent dismantling of the RNA polymerase II elongation complex by the pre-mRNA 3′-end processing factor, Pcf11. *Genes Dev.*, **19**, 1572–1580.
56. Zhang,Z. and Gilmour,D.S. (2006) Pcf11 is a termination factor in Drosophila that dismantles the elongation complex by bridging the CTD of RNA polymerase II to the nascent transcript. *Mol. Cell*, **21**, 65–74.
57. Leipe,D.D., Wolf,Y.I., Koonin,E.V. and Aravind,L. (2002) Classification and evolution of P-loop GTPases and related ATPases. *J. Mol. Biol.*, **317**, 41–72.
58. Burgess,B.K. and Lowe,D.J. (1996) Mechanism of molybdenum nitrogenase. *Chem. Rev.*, **96**, 2983–3012.
59. Gatti,D., Mitra,B. and Rosen,B.P. (2000) *Escherichia coli* soft metal ion-translocating ATPases. *J. Biol. Chem.*, **275**, 34009–34012.
60. Varshavsky,A. (1997) The N-end rule pathway of protein degradation. *Genes Cells*, **2**, 13–28.